



Long-term culture of the marine dinoflagellate microalga *Amphidinium carterae* in an indoor LED-lighted raceway photobioreactor: Production of carotenoids and fatty acids



A. Molina-Miras^a, L. López-Rosales^a, A. Sánchez-Mirón^{a,b}, M.C. Cerón-García^{a,b}, S. Seoane-Parra^{c,d}, F. García-Camacho^{a,b,*}, E. Molina-Grima^{a,b}

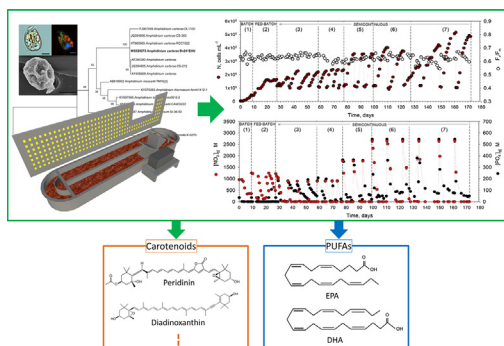
^a Chemical Engineering Area, University of Almería, 04120 Almería, Spain

^b Research Center in Agrifood Biotechnology (BITAL), University of Almería, 04120 Almería, Spain

^c Department of Plant Biology and Ecology, University of the Basque Country (UPV/EHU), P.O. 644, 48080 Bilbao, Spain

^d Technology and Research Centre for Experimental Marine Biology and Biotechnology (PiE-UPV/EHU), Bilbao, Spain

GRAPHICAL ABSTRACT



ARTICLE INFO

Keywords:
Microalgae
Dinoflagellates
Raceway photobioreactor
Amphidinium carterae
Carotenoids
Fatty acids

ABSTRACT

The feasibility of the long-term (> 170 days) culture of a dinoflagellate microalga in a raceway photobioreactor is demonstrated for the first time. *Amphidinium carterae* was chosen for this study as it is producer of interesting high-value compounds. Repeated semicontinuous culture provided to be a robust operational mode. Different concentration levels of the f/2 medium nutrients (i.e. f/2 × 1–3) were assayed. The composition f/2 × 3 (N:P = 5), combined with a sinusoidal irradiance pattern (L/D = 24:0) with a 570 μE m⁻² s⁻¹ daily mean irradiance, maximized the biomass productivity (2.5 g m⁻² day⁻¹) and production rate of the valuable carotenoid peridinin (19.4 ± 1.35 mg m⁻² L⁻¹ with nearly 1% of the biomass d.w.). Several carotenoids and polyunsaturated fatty acids were also present in significant percentages in the harvested biomass (EPA, 1.69 ± 0.31% d.w.; DHA, 3.47 ± 0.24% d.w.), which had an average P-molar formulate of C_{40.7}O_{21.2}H_{73.9}N_{3.9}S_{0.3}P₁.

* Corresponding author at: Chemical Engineering Area, University of Almería, 04120 Almería, Spain.
E-mail address: fgarcia@ual.es (F. García-Camacho).

1. Introduction

Marine dinoflagellate microalgae are a source of numerous fascinating bioactive compounds (Gallardo-Rodríguez et al., 2012; Assunção et al., 2017). However, supply constraints are a major obstacle to the successful research, development and commercialization of compounds from dinoflagellates (Camacho et al., 2007; Gallardo-Rodríguez et al., 2012; Assunção et al., 2017). In this sense, the lack of custom-made methods for successfully culturing dinoflagellates in industrial-scale photobioreactors (PBRs) still represents a hurdle to the production of large amounts of bioactives because of their high sensitivity to damage by hydrodynamic stress (García-Camacho et al., 2014). Recent studies have assessed the feasibility of recovering bioactives (e.g. amphidinols and karlotoxins) from pilot-plant cultures of the dinoflagellates *Amphidinium carterae* and *Karolodinium veneficum* using simple and scalable processes (López-Rosales et al., 2016; López-Rosales et al., 2017; Molina-Miras et al., 2018). The biomass produced in these systems contains significant amounts of other high-value compounds, such as carotenoid pigments and fatty acids, recovery of which would improve the sustainability and economics of these bioprocesses.

A number of carotenoids are produced by marine dinoflagellate microalgae. Peridinin, for example, is a unique marker pigment in most dinoflagellates and has interesting technological applications due to its unique photophysical properties and potential use in medicine as a therapeutic agent against different diseases (Henriksen et al., 2002; Carbonera et al., 2014; Onodera et al., 2014; Ishikawa et al., 2016). In addition, microalgae currently represent a viable alternative source for a wide variety of lipids, with the polyunsaturated fatty acids EPA (eicosapentaenoic acid) and DHA (docosahexaenoic acid) being the most important due to their numerous nutraceutical and pharmaceutical applications (Adarme-Vega et al., 2014). *A. carterae* also produces EPA and DHA (Fuentes-Grunewald et al., 2016).

The biosynthesis of lipids, pigments and polyketide metabolites in microalgae can be tuned by varying operational and abiotic stress factors (Van de Waal et al., 2014; Paliwal et al., 2017). Continuous stress conditions commonly favour the accumulation of these metabolites, but at the expense of significantly reducing their overall productivities, thereby ultimately increasing production costs. To mitigate this problem, a variety of two-stage cultivation strategies have been reviewed (Paliwal et al., 2017). However, the whole culture is generally sacrificed at the end of the second stage. Alternatively, repeated fed-batch and semicontinuous culture modes may be considered to be less detrimental to the overall process yield.

The PBRs used in dinoflagellate-based bioprocesses are typically of the bubble column or flat-panel type (Wang et al., 2015; Fuentes-Grunewald et al., 2016; López-Rosales et al., 2016; López-Rosales et al., 2017; Molina-Miras et al., 2018), such systems being highly compact and providing a high surface to volume ratio. However, as far as we are aware, the use of raceway PBRs to culture dinoflagellate microalgae has never been reported. Raceway PBRs have been used on a wide variety of scales to culture non-dinoflagellate microalgae for diverse applications, with the vast majority of such systems using either sunlight or conventional indoor lighting for illumination rather than light-emitting diodes (LEDs). A few studies have recently demonstrated that dinoflagellates can be successfully cultured in pilot-scale bubble column PBRs illuminated with multi-color LEDs (López-Rosales et al., 2016; Molina-Miras et al., 2018). However, very few previous attempts to culture microalgae in large LED-illuminated raceway PBRs have been reported for non-dinoflagellate species (Husemann et al., 2017).

This work reports on the feasibility of culturing a new strain of the shear-sensitive marine dinoflagellate microalga *Amphidinium carterae* in a pilot-scale LED-illuminated raceway photobioreactor sequentially in batch, fed-batch and semicontinuous modes. Morphological and genetic identification of the strain of *A. carterae* was addressed. Different nutrient concentrations of the f/2 medium were assayed, either by proportionally multiplying all by the same factor (i.e. f/2 × 1, f/2 × 2 and f/

2 × 3) and/or modifying the N:P ratio by increasing the phosphate-P concentration. Three regimes of irradiance (L/D = 12:12, 18:6 and 24:0) were studied in which a sinusoidal diel variation pattern of irradiance was imposed during the illuminated period. By assuming a two-dimensional diffuse incident light model, values of the effective attenuation coefficient of the microalgal suspension and average irradiances inside the culture could be determined. The biomass production capacity of the raceway PBR was analyzed from measurements of elemental composition of *A. carterae* and from phosphorous and nitrogen balances. Culture dynamics were interpreted in terms of the above-mentioned variables and factors. The harvested biomass was evaluated in terms of carotenoid pigments and fatty acid content.

2. Materials and methods

2.1. Maintenance of the microalga and inocula

Amphidinium carterae was isolated by pipetting from a water sample collected in the Mediterranean Sea (Palma de Mallorca, close to Punta des Gas, Spain) and deposited in the microalgae culture collection of the Plant biology and Ecology Department of The University of the Basque Country as *Amphidinium carterae* Dn241EHU. The morphological and genetic identification can be found in the article for Data in Brief. *A. carterae* is a shear- and bubbling-sensitive microalga and inocula were grown in f/2 medium as described elsewhere (Molina-Miras et al., 2018). The original composition of the f/2 medium has an N:P molar ratio of 24.

2.2. Cultivation in the LED-based raceway PBR

A. carterae was cultured in a fiberglass paddlewheel-driven raceway PBR with semicircular ends and a surface area of 0.44 m². Curved baffles installed at either end ensured a uniformity of flow through the curved bend and minimized the formation of dead zones. The raceway channel below the paddlewheel was flat. The PBR was operated at a culture depth of 7.5 cm (equivalent to a 33 L culture volume) to minimize light attenuation. A six-bladed paddlewheel with flat blades was used at a rotation speed of 23.1 ± 0.6 rpm, moving the culture at a flow rate of 20.7 ± 0.3 cm s⁻¹. The flow rate was measured using the basic tracer method (Sánchez Mirón et al., 2000). Further details of the culture system are provided in Fig. 1. The RW-PBR was illuminated using multicolor LED strips (red, green, blue and warm white, collectively referred to as RGBW; Edison Opto Co., Taiwan) similar to those used in recent studies with dinoflagellate microalgae (López-Rosales et al., 2016; Molina-Miras et al., 2018). These LED strips were attached horizontally on the back of a flat plastic (PVC) cover placed on the PBR. Water losses due to evaporation were compensated at the same rate by

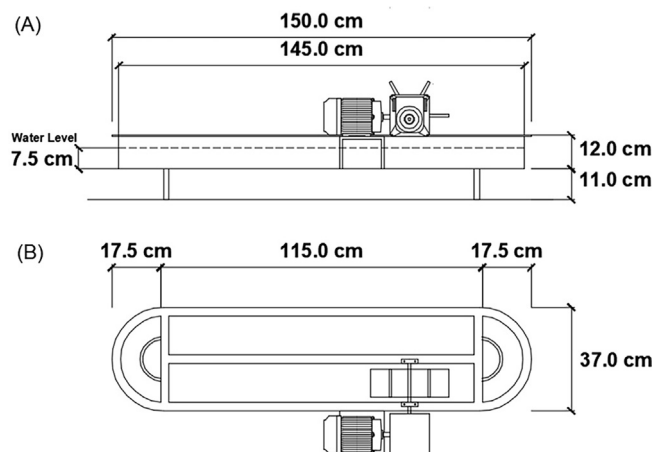


Fig. 1. The raceway photobioreactor. (A) Side and (B) top views.

automatically adding the required volume of sterile distilled water with a peristaltic pump actioned by a level sensor. This operational mode allowed for keeping the culture volume fixed at 33 L. The evaporation rate depended on the irradiance regime used, the air temperature and the absolute humidity. An average freshwater evaporation rate of $3.34 \text{ L m}^{-2} \text{ day}^{-1}$ was measured. The pH was maintained at 8.5 by automatically injecting pure carbon dioxide, as needed by the cells, through a small microporous gas diffuser in the form of fine bubbles. This carbon dioxide diffuser was placed at the bottom, immediately behind the paddlewheel. The culture temperature was maintained at $21 \pm 1^\circ \text{C}$ by circulating thermostated water through a 4.6 m stainless steel tubular loop (6 mm inner and 8 mm outer diameters) located at the bottom of the channels. *A. carterae* satisfactorily endured the operational conditions set up in the raceway PBR. Photosynthetic efficiency and cytometric measurements carried out routinely in inocula grown in static T-flasks and the raceway culture did not present significant differences, indicating absence of shear damage in the raceway PBR. This is in line with literature published on PBRs. As agitation levels in raceway ponds are very low ($< 1 \text{ W/m}^3$) compared to bubble column PBRs ($< 100 \text{ W/m}^3$), shear stress from mixing is not a significant concern in this kind of culture systems. On the other hand, these ponds are much shallower ($< 20 \text{ cm}$) than bubble column PBRs (around 2 m), and therefore shear stress associated with bubbling is also negligible.

$f/2$ medium was used as a basis for assaying different nutrient concentrations either by proportionally multiplying all by the same factor (i.e. $f/2 \times 1$, $f/2 \times 2$ and $f/2 \times 3$) and/or decreasing the N:P ratio from 24 for $f/2 \times 1$ medium to 5 by increasing the phosphate-P concentration. All culture media were prepared using filter-sterilized Mediterranean seawater and then autoclaved. Three culture modes were assayed with this temporal sequence: batch, fed-batch mode with a pulse feeding strategy and semicontinuous mode. The experiment started with a batch culture phase in which the $f/2$ medium (30 L) was inoculated with 3 L of an inoculum containing algal cells in the late exponential growth phase. The cell concentration in the freshly inoculated photobioreactor was around $3.1 \times 10^4 \text{ cells mL}^{-1}$. In fed-batch mode, concentrated medium stocks were added every time a stationary growth phase was reached. For this, 1 L of culture was replaced by an equal volume containing a nutrient stock equivalent to 33 L of the medium used. Once pulses of nutrient stock did not increase the cell concentration, a semicontinuous mode was explored until the end of the study. Semicontinuous operation consisted in removing a variable culture volume and replenishing with an equal volume of fresh medium. Each replenishment was carried out once the culture entered a stationary phase. Each time, and after measuring phosphate and nitrate in the supernatant, the fresh medium was supplemented with phosphate and nitrate stock solutions so that the final concentrations of these nutrients in the whole culture volume ($= 33 \text{ L}$) were close to the values established for the medium formulation selected (i.e. $f/2 \times 1$, $f/2 \times 2$ or $f/2 \times 3$). The other remaining nutrients were added in equivalent quantities to those of the medium formulation selected. Semicontinuous culture was repeated several times for each experimental combination evaluated (i.e. medium formulation and illumination regime). After every replenishment, a cell concentration of about $10^6 \text{ cell mL}^{-1}$ was fixed as baseline in all sets in semicontinuous mode. The complete operational strategy is summarized in detail in Table 1, where an explanation of the intervals for each experimental set is also provided.

A sinusoidal diel variation pattern of irradiance was imposed using the following equation (López-Rosales et al., 2016; Molina-Miras et al., 2018):

$$I_0(t) = \begin{cases} I_{\text{max}} \sin \left[\pi \frac{t - t_{\text{sr}}}{t_{\text{ss}} - t_{\text{sr}}} \right] & \text{if } t_{\text{sr}} \leq t \leq t_{\text{ss}} \\ 0 & \text{otherwise} \end{cases} \quad (1)$$

where I_{max} is the maximum irradiance occurring at midday; t_{sr} is the

time of sunrise; and t_{ss} is the time of sunset. The PBR was operated under three illumination regimes given by Eq. (1), as described below. The value of I_{max} in Eq. (1) was first measured at the bottom of the photobioreactor filled only with seawater. Measurements were performed at different axial locations along the central axis of the channel. A relatively low average I_{max} of $300 \mu\text{E m}^{-2} \text{ s}^{-1}$ was fixed for the first four days of the batch culture phase (Set 1) in order to facilitate acclimation of the inoculum. The I_{max} value for the rest of the culture time was $900 \mu\text{E m}^{-2} \text{ s}^{-1}$. Irradiance values were measured using a spherical quantum sensor (Biospherical QSL 100; Biospherical Instruments Inc., San Diego, CA, USA). A two-dimensional diffuse incident light scenario in which irradiance did not vary significantly along the axial axis of the channel can be assumed with this kind of LED setup (López-Rosales et al., 2016; Molina-Miras et al., 2018). Therefore, and assuming the attenuation of irradiance inside the culture complies with the Beer-Lambert law for homogeneous media, the total irradiance reaching a point at the bottom from all directions contained in the axial plane of the channel can be calculated using the following equation:

$$I(L, t) = \frac{I_0(t)}{\pi} \int_{-\pi/2}^{\pi/2} e^{-\kappa(t) \frac{L}{\cos(\beta)}} d\beta \quad (2)$$

In Eq. (2), L is the depth of the culture, $I(L, t)$ is the irradiance at the bottom at any time t during culture; $I_0(t)$ is the irradiance determined according to Eq. (1) at the bottom of the PBR filled with the culture medium; β is the angle of penetration of the incident light beam in the axial plane of the channel; and $\kappa(t)$ (m^{-1}) is the effective attenuation coefficient of the microalgal suspension averaged over the PAR wavelengths. Eq. (2) was used to determine $\kappa(t)$ from measurements of $I(L, t)$ at different cultures times. Thus, the local irradiance at a depth x can be estimated at any instant by

$$I(x, t) = \frac{I_0(t)}{\pi} \int_{-\pi/2}^{\pi/2} e^{-\kappa(t) \frac{x}{\cos(\beta)}} d\beta \quad (3)$$

In this case, $\kappa(t)$ is related to the effective light attenuation across a cell averaged over the PAR wavelengths, $\alpha(t)$ ($\text{m}^2 \text{ cell}^{-1}$), and the cell number concentration, N (cells m^{-3}), by the following equation (López-Rosales et al., 2016):

$$\kappa(t) = \alpha(t) \cdot N(t) \quad (4)$$

Thus Eq. (4) allows us to obtain $\alpha(t)$. Values for the average irradiance inside the culture ($I_{\text{av}}(t)$, $\mu\text{E m}^{-2} \text{ s}^{-1}$) were estimated using the following equation:

$$I_{\text{av}}(t) = \frac{1}{L} \int_0^L I(x, t) dx \quad (5)$$

The daily mean I_{av} (i.e. Y_{av}) values for any given day were calculated as follows:

$$Y_{\text{av}} = \frac{1}{24} \int_{t_{\text{sr}}}^{t_{\text{ss}}} I_{\text{av}}(t) dt \quad (6)$$

As indicated in Table 1, the three diel variation patterns of irradiance assayed were the following: (i) 12:12; (ii) 18:6; and (iii) 24:0. That is, LEDs were turned on in the timeslots ($t_{\text{sr}} - t_{\text{ss}}$) 6:00–18:00 h, 6:00–24:00 h and 6:00–6:00 h, respectively. Equation applied at $\kappa = 0$ (i.e. culture without cells) provides the daily mean irradiance Y_0 supplied to the culture medium. The value of Y_0 was calculated for each of the diel variation patterns of irradiance used in this study (see Table 1).

2.3. Other analytical measurements

The cell number concentration (N) and average cell diameter were quantified by flow cytometry, as described elsewhere (López-Rosales et al., 2016). Five measurements per sample were performed and the average value was used. The biomass dry weight was determined as described previously (Molina-Miras et al., 2018). All experiments were performed in triplicate. Two biomass concentration calibration curves

Table 1

The strategy used in this study. Seven experimental sets were defined in terms of the culture mode, the daily mean irradiance Y_o received by the culture (given by Eq. (6) at $\kappa = 0$), composition and N:P molar ratio of the culture medium. The specific intervals for each culture mode are included. The column labelled nutrients describes stock solutions for fed-batch mode and the initial composition of the culture medium in the semicontinuous mode. The percentages of replenished culture volume in semicontinuous mode are also shown. The maximum irradiance occurring at midday, I_{omax} , appears in Eq. (1). $[\text{NO}_3^-]_o$, $[\text{PO}_4^{3-}]_o$ and (N:P)_o represent nitrate and phosphate concentrations and nitrogen to phosphorous molar ratio in the culture medium respectively.

Set	Interval (days)	Culture mode	I_{omax} , $\mu\text{Em}^{-2}\text{s}^{-1}$	L/D cycle, hours	Y_o , $\mu\text{Em}^{-2}\text{s}^{-1}$	$[\text{NO}_3^-]_o$, μM	$[\text{PO}_4^{3-}]_o$, μM	(N:P) _o	Replenished volume (%)	Nutrients
1	0–4	Batch	300	12:12	100	882	36,2	24	–	f/2 × 1
	5–9		900		286					–
2	9–14	Fed-batch	900	12:12	286	882	36,2	24	–	f/2 × 1 (165 mL stock solution)
	14–20									f/2 × 1 (165 mL stock solution)
	20–22									f/2 × 1 (165 mL stock solution)
	22–24									f/2 × 1 (165 mL stock solution)
	24–27					882	108,6	8	–	(PO_4^{3-}) _{f/2} × 3 (100 mL stock solution)
3	27–29	Semicontinuous	900	12:12	286	882	36,2	24	20	f/2 × 1
	29–36					882	181	5	10	f/2 × 1; [PO_4^{3-}] _{f/2} × 5
	36–43								30	
	43–51								50	
	51–58								40	
4	58–64			18:6	430					45
	64–69									45
	69–73									45
	73–77									45
5	77–85			18:6	430	1764	362	5	45	f/2 × 2; [PO_4^{3-}] _{f/2} × 10
	85–92								60	
	92–99								60	
6	99–110			18:6	430	2646	529	5	60	f/2 × 3; [PO_4^{3-}] _{f/2} × 14.6
	110–122								70	
	122–127								–	
7	127–134			24:0	573				55	
	134–149								70	
	149–161								75	
	161–172								75	

were determined. One of them expressed as dry weight (C_b) versus optical density at 720 nm (OD720): C_b (gL^{-1}) = $1.012 \times \text{OD720}$ ($r^2 = 0.926$; $n = 56$). The other one as dry weight (C_b) versus cyto-metric biovolume of cells per mL of culture (V_c): C_b (gL^{-1}) = $0.176 \times N \times V_c$ ($r^2 = 0.877$; $n = 56$). Biomass (d.w.) and cell productivities were calculated in terms of culture volume (i.e. volumetric values) and occupied area (i.e. areal productivities). The ratio between the maximum variable fluorescence (F_v) and the maximum fluorescence (F_m) of chlorophyll (i.e. F_v/F_m) in cells was routinely determined as described previously (López-Rosales et al., 2015). Total phosphorus (P_T) and nitrogen (N_T) in biomass and supernatants and phosphate-P and nitrate-N in supernatants were determined as described in a recent study (Molina-Miras et al., 2018). Measurements were carried out in duplicate samples and average value was used.

The elemental composition of the biomass was determined as published previously (Molina-Miras et al., 2018), with only atoms found in the main macromolecules (C, O, N, H, S, P) being taken into account. Measurements were carried out in duplicate. NOCHSP analysis was carried out for the biomass harvested in the semicontinuous culture in Sets 3–7 (see Table 1). The potentially growth-limiting macronutrients in the culture medium were nitrate-N and phosphate-P. Carbon and sulfur were present in excess (Molina-Miras et al., 2018). The theoretical maximum biomass concentration (C_{bmax}) for nitrate-N and phosphate-P from the culture medium was calculated as described previously (Molina-Miras et al., 2018). The element (nitrate-N or phosphate-P) producing the smallest C_{bmax} is considered to be the growth-limiting nutrient. The fatty acid (FA) content and profile were obtained by direct transesterification and gas chromatography (6890 N Series Gas Chromatograph, Agilent Technologies, Santa Clara, CA, USA) as described by Rodríguez-Ruiz et al. (Rodríguez-Ruiz et al., 1998).

Measurements were carried out in duplicate.

The pigment content and profile in cells were determined using an HPLC apparatus equipped with a diode array detector, as explained in Seoane et al. (Seoane et al., 2009), following the method described in Zapata et al. (Zapata et al. 2000). Pigments were identified on the basis of their retention times and absorbance spectra. Retention times were compared with those of pure standards obtained commercially from DHI (Hoersholm, Denmark) and those reported elsewhere (Jeffrey, 1997; Zapata et al., 2000). HPLC calibration was performed using the external standards provided by DHI (chlorophylls a, b and c2, and carotenoids fucoxanthin, lutein, zeaxanthin and peridinin). The molar extinction coefficients reported in the literature were used to quantify those carotenoids not calibrated using commercial standards (Jeffrey, 1997). Measurements were carried in duplicate using cultures samples of 10 mL.

2.4. Statistical analyses

Multifactor ANOVAs and non-linear regression analyses were performed using Statgraphics Centurion XVI (StatPoint, Herndon, VA, USA).

3. Results and discussion

3.1. Culture experiment in the PBR

A representative culture profile for the LED-illuminated RW-PBR is displayed in Fig. 2. The F_v/F_m value did not change significantly during culture, with the average value of 0.625 ± 0.023 being indicative of healthy cells throughout the culture time (Fig. 2A). The cell diameter

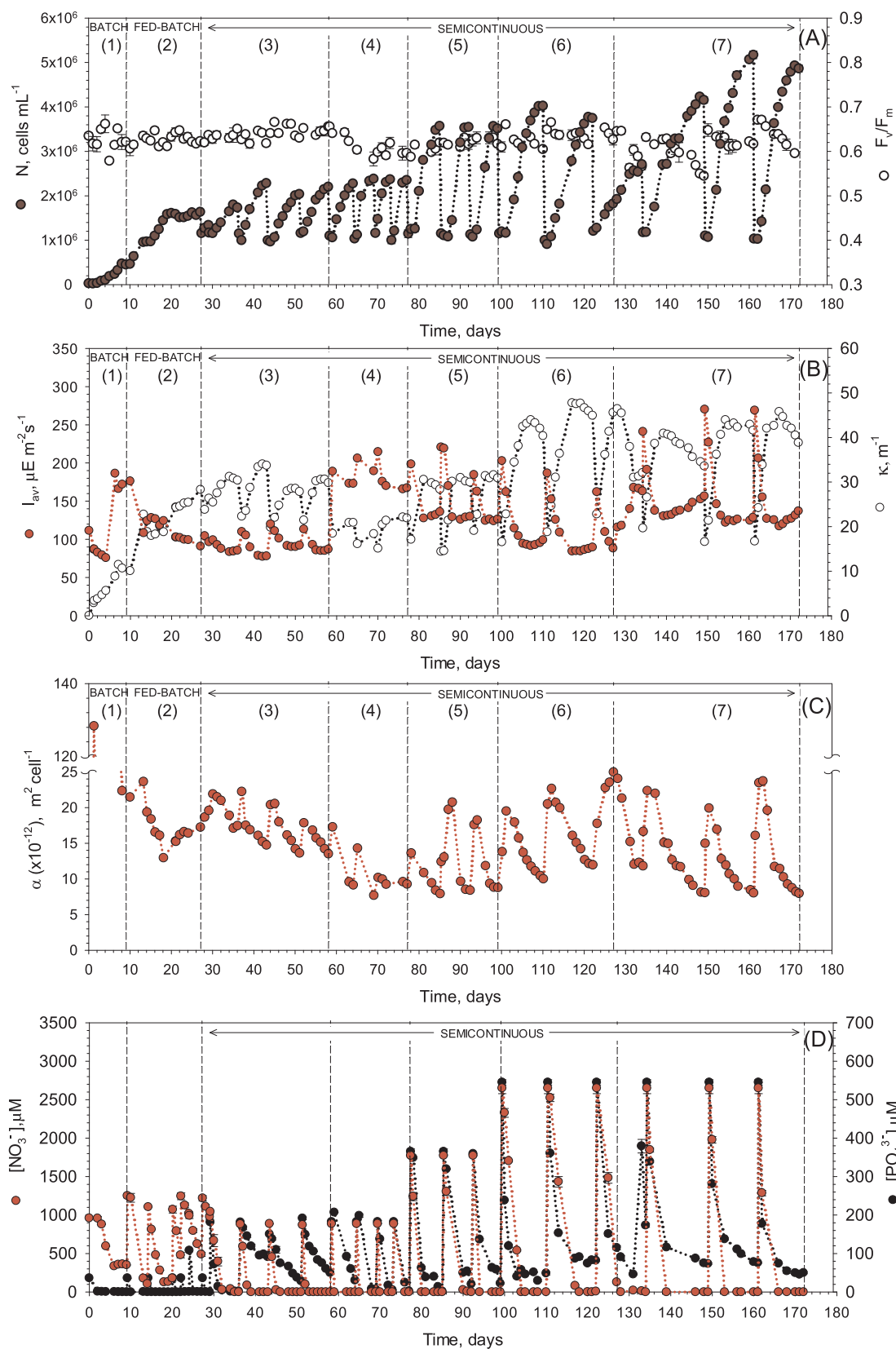


Fig. 2. Dynamics for sequential culture of the microalga *Amphidinium carterae* in the pilot-scale LED-illuminated raceway photobioreactor. Temporal changes in (A) the cell concentration (N) and maximum photochemical yield of photosystem II (F_v/F_m); (B) average irradiance available for the cells (I_{av}) and effective attenuation coefficient of the microalgal suspension (κ); (C) effective light attenuation across a cell (α); (D) dissolved nitrate ($[NO_3^-]$) and phosphate ($[PO_4^{3-}]$) concentrations in the supernatant are shown. The vertical dotted lines delimit the different experimental sets performed according to the strategy described in Table 1. Data points are averages, and vertical bars are standard deviations (SD) for duplicate samples.

averaged throughout the culture time was $12.37 \pm 1.09 \mu\text{m}$ ($n = 711$). However, fluctuations in cell diameter, ranging from a minimum of $10.70 \pm 0.15 \mu\text{m}$ to a maximum of $15.53 \pm 0.06 \mu\text{m}$, were observed, thus implying significant changes in cell biovolume from 641 ± 27 to $1961 \pm 23 \mu\text{m}^3$, respectively. Set 1 commenced as a batch culture (Set 1) with an initial Y_o value of $100 \mu\text{E m}^{-2} \text{s}^{-1}$ to allow the inoculum cells to adapt to the new conditions in the LED-PBR. After four days, Y_o was increased to $286 \mu\text{E m}^{-2} \text{s}^{-1}$ and maintained for the rest of the Set. A stationary phase was attained after 9 days in Set 1 with an N value of around $4.5 \times 10^5 \text{ cells mL}^{-1}$ (equivalent to $0.12 \text{ g d.w. L}^{-1}$) (Fig. 2A). As can be seen in Fig. 2D, rapid depletion of dissolved phosphate-P in the supernatants seemed to be the cause. Indeed, phosphate-P was rapidly taken up soon after being added, whereas nitrate-N continued to be present in excess. As illustrated in Fig. 2D, this phosphate-P limitation was confirmed by repeatedly replenishing the culture, as specified in Table 1 for Set 2. In contrast, nitrates gradually accumulated in the culture. Obviously, the quantity of cells and biomass gained by the culture decreased with each replenishment (or stage), since the availability of phosphate per cell diminished markedly as cell concentration (N) increased with culture time. This dynamics is similar to that reported for *A. carterae* and *K. veneticum* grown in bubble-column PBRs (López-Rosales et al., 2016; Molina-Miras et al., 2018). Despite the repeated additions of nutrients performed in Set 2, there was no growth beyond day 20. Possible light-limited growth was ruled out since the average irradiance available for the cells (I_{av}) (see Fig. 2B) was above the basal value and could sustain a higher cell concentration in the culture, as demonstrated subsequently in the semi-continuous culture. From days 20–24, the repeated additions of $f/2$ stock solutions were insufficient to support even a stationary growth phase. However, the single addition of phosphate-P on day 24 of culture led to a slight increase in cell concentration until day 27. Apparently, fed-batch culture using the high N:P ratio (=24) of the $f/2$ medium meant that phosphorus became a limiting nutrient and strong growth regulator, thereby not allowing a balanced and sustained growth.

From day 27 different semi-continuous cultures (sets 3–7 in Table 1) were carried out with an N:P ratio in the replenished fresh medium of 5. In all cases the final cell concentration (N_f) achieved increased progressively as both Y_o and/or the concentration of nutrients based on the nutrient proportion in the $f/2$ medium (i.e. $f/2 \times i$) increased. The dynamics of N , I_{av} , and nitrate and phosphate concentrations in the supernatants followed a consistent pattern typical of semicontinuous cultures in which batch cultures are repeated sequentially (Fig. 2). In all sets, N increased as nitrate and phosphate in the medium were consumed by the cells (see Fig. 2). Likewise, I_{av} decreased sharply due to the increase in the mutual shading between cells, which is consistent with an increase in κ since this is directly proportional to N (see Eq. (4)). However, during the deceleration phase of growth, κ decreased over time even though N continued to increase, thus implying a slight increase in I_{av} . The corresponding values of α represented in Fig. 2C were calculated using Eq. (4). It can be seen that α began to decrease a few days after the beginning of each batch. The dynamics of α paralleled the evolution of nitrates and phosphates in the supernatant (Fig. 2C and D). In other words, α decreased when nutrients began to clearly limit growth. This observation is in good agreement with earlier results reported for cultures of other microalgae in which absorption cross-sections of microalgae strongly decreased upon nitrogen limitation of growth (Reynolds et al., 1997). The variation of α with culture time could therefore be caused by acclimation of cells to changes in light and nutrient availability from Set 3–7 and during the batch-growth phase of each Set. In fact, nitrogen limitation is known to modify the pigment packaging in cells and/or the abundance of accessory light-harvesting pigments (Reynolds et al., 1997), as discussed below.

Fig. 3 shows the effect of the combinations of culture conditions in Sets 3–7, carried out in semicontinuous culture mode, on different kinetic variables such as N_f and biomass productivities (P_b), as expressed in terms of cells or biomass dry weight. To mitigate the potential effects

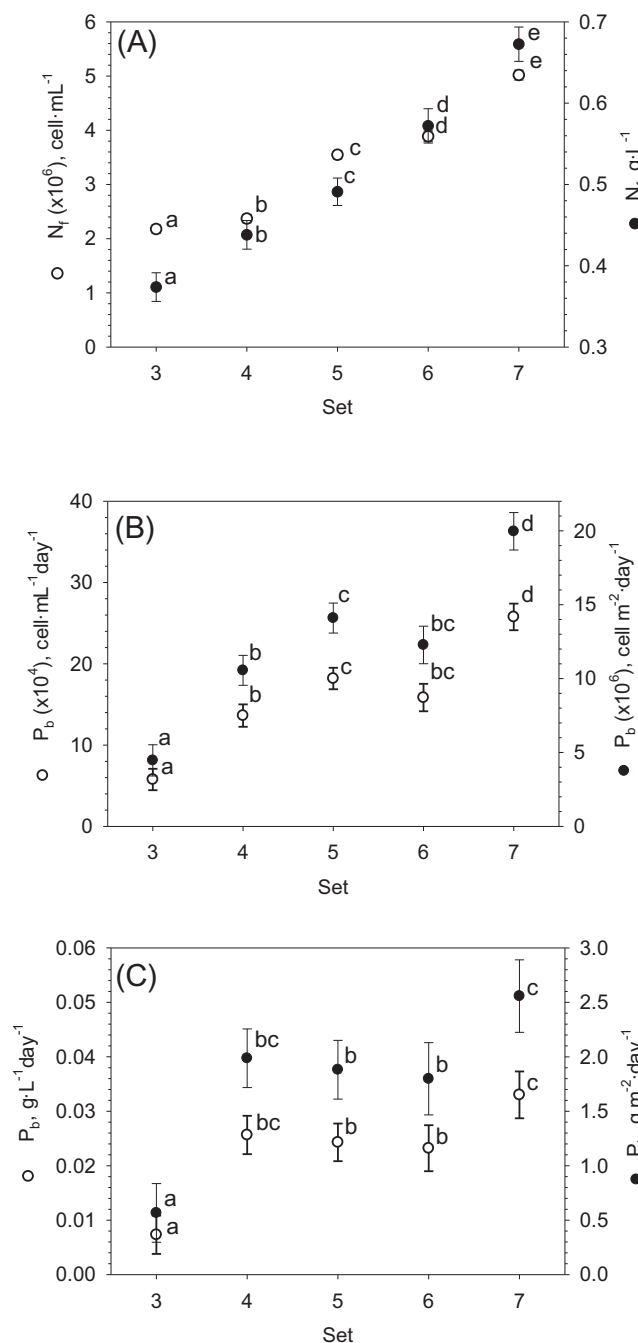


Fig. 3. Effect of irradiance level and culture medium composition on (A) the final cell and biomass concentration (N_f), (B) volumetric and areal cell productivities (P), and (C) volumetric and areal biomass productivities (P) in the different semicontinuous cultures (experimental sets from 3 to 7). Sets 3 and 4: effect of the daily mean irradiance supplied to the culture, Y_o ($Y_{o3} = 286 \mu\text{E m}^{-2} \text{s}^{-1}$; $Y_{o4} = 430 \mu\text{E m}^{-2} \text{s}^{-1}$) using $f/2 \times 1$ at an N:P ratio of 5 as culture medium. Sets 6 and 7: effect of Y_o ($Y_{o6} = 430 \mu\text{E m}^{-2} \text{s}^{-1}$; $Y_{o7} = 573 \mu\text{E m}^{-2} \text{s}^{-1}$) using $f/2 \times 3$ (N:P = 5) as culture medium. Sets 4, 5 and 6: effect of the proportion of $f/2$ nutrients added (i.e. $f/2 \times 1$, $\times 2$ and $\times 3$) at a Y_o of $430 \mu\text{E m}^{-2} \text{s}^{-1}$. Data points are averages and values denoted by a different lowercase at each point differ significantly ($p < 0.05$) in the one-way ANOVA. Bars around points represent 95% confidence intervals based on Fisher's least significant difference (LSD) procedure. Overlapping bars indicate no significant difference.

of acclimation in cells when changing from one experimental set to another, the data represented in Fig. 3 were calculated using the measurements of the last two semicontinuous cultures for each set. For

comparison purposes, the following combinations of sets were selected on the basis of the effect of the factors explored with them (see Table 1): (i) sets 3 and 4 were used to compare the effect of Y_o corresponding to the irradiance diel variation patterns of 12:12 and 18:6, respectively, using $f/2 \times 1$ (N:P = 5) as culture medium; (ii) sets 6 and 7 were used to compare the effect of Y_o corresponding to the irradiance diel variation patterns of 18:6 and 24:0, respectively, using $f/2 \times 3$ (N:P = 5) as culture medium; (iii) sets 4, 5 and 6 were used to evaluate the effect of the proportion of $f/2$ nutrients added (i.e. $f/2 \times 1$, $\times 2$ and $\times 3$) at a fixed value of Y_o . As can be seen from Fig. 3A, N_f increased progressively throughout the experimental run, with maximum values of around 5×10^6 cell mL⁻¹ and 0.67 gL⁻¹ being achieved in the last set. On average, N_f was improved by 172% (based on cells) and 221% (based on biomass dry weight) relative to Set 3, and 931% and 771% relative to Set 1. The differences in these percentages can be attributed to differences in the average cell size throughout the culture time. Indeed, the cell concentration and biomass dry weight did not correlate well, whereas the opposite was found for the culture biovolume (see Materials and Methods section). As regards biomass productivity, the P_b values improved significantly upon increasing Y_o from 286 (Set 3) to $430 \mu\text{E m}^{-2} \text{s}^{-1}$ (Set 4), using $f/2$ medium at N:P = 5. The light availability for cells increased in Set 4 compared to Set 3 due to a reduction in the effective light attenuation across a cell (α) averaged in Set 4 relative to Set 3 (see Fig. 2C). In contrast, the P_b values did not suffer substantial changes when multiplying the concentrations of all nutrients by up to 3 (Sets 4–6), remaining constant at an $(\text{N:P})_{\text{medium}}$ of 5 and Y_o of $430 \mu\text{E m}^{-2} \text{s}^{-1}$ (Fig. 2B and C). The positive effect of increasing N_f resulting from the higher availability of nutrients from Set 4–6 was, in turn, neutralized by the slight increase in mutual cell shading observed (i.e. increase of the average α value for each Set (see Fig. 1C)). This negative effect was reverted in Set 7 by increasing Y_o and medium nutrients up to $573 \mu\text{E m}^{-2} \text{s}^{-1}$ and $f/2 \times 3$, respectively. The values of P_b and N_f increased again markedly. All the increases and decreases in α observed in Fig. 2C were consistent with the corresponding changes measured in the cell pigments, as discussed below. In summary, the maximum P_b values were achieved in the last set: 25.8×10^4 cell mL⁻¹ day⁻¹ or 19×10^6 cell m⁻² day⁻¹ (Fig. 3B) and 0.033 gL⁻¹ day⁻¹ or 2.5 g m⁻² day⁻¹ (Fig. 3C). This represents an almost 4.5-fold improvement from set 3 to set 7.

3.2. Biomass capacity based on the elemental composition of *A. carterae*

The total amount of biomass dry weight produced by the PBR was 169.3 g (d.w.). Since the elemental composition of the biomass varied slightly among the different experimental sets, although not systematically, a weighted average elemental composition of 48.8 ± 0.2 (C%), 33.8 ± 0.3 (O%), 7.5 ± 0.1 (H%), 5.2 ± 0.1 (N%), 1.0 ± 0.1 (S%), 3.2 ± 0.1 (P%) was calculated ($n = 38$) for the whole biomass obtained. This means that the phosphate-P and nitrate-N quantities actually fixed in the biomass were 5.24 ± 1.01 and 9.13 ± 2.37 g, respectively. All replenishments of culture medium accounted for phosphate-P and nitrate-N quantities of 5.97 and 15.11 g, respectively. If, in addition, the quantity of phosphorous (0.54 g) and nitrogen (0.81 g) withdrawn in the supernatants of the samples and the culture harvested in Sets 3–7 is taken into account, the phosphate-P and nitrate-N theoretically fixed in the biomass should have been 5.43 g and 14.3 g, respectively. These estimations differ from the experimental values by less than 4% for phosphorous and 36% for nitrogen. Given these amounts and the average elemental composition described above, the maximum biomass yields that could theoretically be supported would be 169.81 and 275.14 g (d.w.) for phosphate-P and nitrate-N, respectively. According to these estimations, phosphate-P was the main growth-limiting nutrient. This result is consistent with the phosphate-P profile in the culture supernatant observed in Fig. 2D, where $[\text{PO}_4^{3-}]$ is always close to being exhausted in all sets. In contrast, nitrate-N in the supernatants was exhausted before phosphates in Sets 3–7 even though

nitrate-N was apparently in excess, as also demonstrated by the cell N:P molar ratio of 3.9 calculated from the average biomass elemental composition. In light of this observation, the lost nitrate-N is likely to have been incorporated into forms other than the suspended culture. That is, there must be another small sink of nutrients incorporating N and P. The main candidate seems to be the biofouling layer of *A. carterae* developed on various parts of the PBR. Photographs of the newly emptied PBR taken after 249 days of culture support this hypothesis. Although the *A. carterae* biomass forming part of biofouling could not be accurately measured, it seems plausible that the actual biomass generated by the PBR was somewhat higher than the 169 g determined experimentally, thus being closer to the 275 g expected theoretically if nitrate-N was the growth-limiting nutrient. Irrespective of this, the results seem to indicate that both nitrate-N and phosphate-P in the culture medium were growth co-limiting.

The corresponding average P-molar formula derived from the above average biomass elemental composition was $\text{C}_{40.7}\text{O}_{21.2}\text{H}_{73.9}\text{N}_{3.9}\text{S}_{0.3}\text{P}_1$, with the molar ratios C:P = 40.7, C:N = 10.4 and N:P = 3.9. Literature data reveal a marked variability for microalgae, and significant variations in these ratios have been reported for dinoflagellates (C:P = 36–166, C:N = 5–11.3 and N:P = 5.5–23) (Leonardos and Geider, 2004). This variability in the macronutrient (C:N:P) stoichiometry was associated with both phylogenetic differences and the wide range of growth conditions used (Leonardos and Geider, 2004). In general, abiotic factors that may affect the elemental composition of microalgae include nutrient concentration ratios, light phase length, irradiance level, salinity or temperature, and several studies have confirmed this unpredictability in the case of *A. carterae*. For example, when cultured at different irradiances ranged from 15 to $500 \mu\text{E m}^{-2} \text{s}^{-1}$, the strain *A. carterae* Hulburt presented minimum values for the C:P (= 105) and N:P (= 4.1) ratios at the intermediate irradiance of $100 \mu\text{E m}^{-2} \text{s}^{-1}$ and average maximum values of 180 and 23, respectively, at the limits of the irradiance range assayed (Finkel et al., 2006). In contrast, the C:N ratio (= 26) reached a maximum at the same intermediate irradiance and a minimum (C:N \approx 7.6) at the limits of the irradiance range (Finkel et al., 2006). In another study, the C:P, C:N, and N:P ratios for *A. carterae* Hulburt varied by less 35%, 14% and 9%, respectively, when cultured at medium N:P ratios ($(\text{N:P})_{\text{medium}}$) ranging from 4 to 20; an average C:N:P ratio of 167:23:1 was determined (Sakshaug et al., 1983). However, when grown at an $(\text{N:P})_{\text{medium}}$ of 10, *A. carterae* presented a C:N:P ratio of 37:4.1:1 (Parsons et al., 1961), similar to that found in this work. On the other hand, when cultured at different $(\text{N:P})_{\text{medium}}$ values (between 10 and 40), the strain *A. carterae* BAHME54 only presented a significant variation in the C:P ratio (112–181), whereas C:N and N:P remained virtually constant at around 7.8 and 18, respectively (Sakshaug et al., 1984). In contrast, the C:N ratio of the strain *A. carterae* ACRNO3 grown under an $(\text{N:P})_{\text{medium}}$ of 24 fluctuated non-systematically in the range 3.3–11.7 (Fuentes-Grunewald et al., 2016). More recently, the same strain showed a P-molar formula of $\text{C}_{326}\text{O}_{126}\text{H}_{732}\text{N}_{69}\text{S}_3\text{P}_1$, which is consistent with a growth strongly regulated by phosphate-P availability in the culture medium ($(\text{N:P})_{\text{medium}} = 88$) (Molina-Miras et al., 2018). Methodological differences between studies may also have contributed to the variability described in the above survey. For example, it has also been demonstrated that microalgae markedly alter their C:N:P ratios as a result of changes in the culture pH since the availability of dissolved CO₂ is modified (Burkhardt et al., 1999). As a result, it is impossible to establish a unique elemental formula for any microalga.

3.3. Pigments

Fig. 4 displays the cell pigment contents, pigment percentage by dried biomass weight and pigment titers in the cultures for experimental Sets 3–7 carried out in semicontinuous mode (data represented in Fig. 4 were also calculated from the measurements of the last two semicontinuous cultures for each set, as mentioned above for Fig. 3).

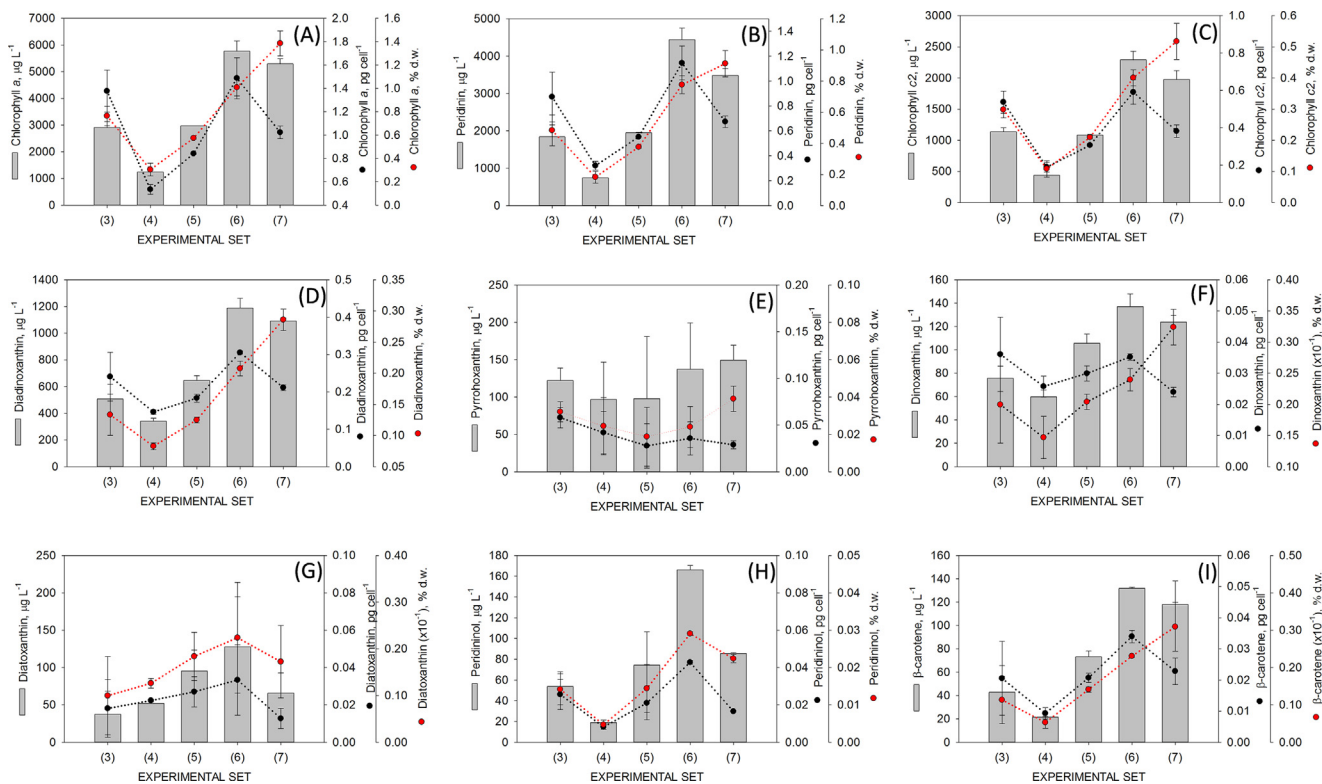


Fig. 4. Effect of irradiance level and culture medium composition on the pigment content expressed in terms of broth titer ($\mu\text{g L}^{-1}$), cell specific content (pg cell^{-1}) and percentage biomass dry weight (% d.w.). (A) Chlorophyll a; (B) Peridinin; (C) Chlorophyll c2; (D) Diadinoxanthin; (E) Pyrrhoxanthin; (F) Dinoxanthin; (G) Diatoxanthin; (H) Peridininol; (I) β -carotene; (J) Diadinochrome. Sets 3 and 4: effect of the daily mean irradiance supplied to the culture, Y_o ($Y_{o3} = 286 \mu\text{E m}^{-2} \text{s}^{-1}$; $Y_{o4} = 430 \mu\text{E m}^{-2} \text{s}^{-1}$) using $f/2 \times 1$ at an N:P ratio of 5 as culture medium. Sets 6 and 7: effect of Y_o ($Y_{o6} = 430 \mu\text{E m}^{-2} \text{s}^{-1}$; $Y_{o7} = 573 \mu\text{E m}^{-2} \text{s}^{-1}$) using $f/2 \times 3$ (N:P = 5) as culture medium. Sets 4, 5 and 6: effect of the proportion of $f/2$ nutrients added (i.e. $f/2 \times 1$, $\times 2$ and $\times 3$) at a Y_o of $430 \mu\text{E m}^{-2} \text{s}^{-1}$. Data points are averages, and vertical bars are standard deviations.

Although the pigment composition showed important differences among sets, all samples analyzed contained diadinochrome, β -carotene, peridininol, diatoxanthin, dinoxanthin, pyrrhoxanthin, diadinoxanthin, chlorophyll c2, peridinin and chlorophyll a. This pigment profile is consistent with that for the peridinin-containing dinoflagellate microalgae defined as Type 1 (Dinophyta) by Jeffrey and Wright (Jeffrey and Wright, 2006), with *chl-a* as major pigment and peridinin as the major carotenoid. In fact, *A. carterae* has been recommended as a source of pigments to produce standards (Jeffrey and Wright, 2006). The variation range of the pigment cell quotas (pg cell^{-1}) measured (see Fig. 4) were in line with data previously reported for *A. carterae* (Ruivo et al., 2011). The total pigment yields, expressed as percentage of biomass dry weight, ranged from $0.75 \pm 0.15\%$ for Set (4) to $3.26 \pm 0.29\%$ for Set (7). Carotenoids accounted for between $0.33 \pm 0.07\%$ and $1.34 \pm 0.13\%$ of the biomass dry weight. The lowest value was similar to that reported for two strains of *A. carterae* grown under different culture conditions and with a different medium composition to those used in this study (Johansen et al., 1974).

Pigment concentrations on a per cell basis decreased systematically as Y_o increased from $286 \mu\text{E m}^{-2} \text{s}^{-1}$ in set 3 to $430 \mu\text{E m}^{-2} \text{s}^{-1}$ in set 4 and from $430 \mu\text{E m}^{-2} \text{s}^{-1}$ in set 6 to $573 \mu\text{E m}^{-2} \text{s}^{-1}$ in set 7 (see Fig. 4). This pattern of photoacclimation regulating the size of the light-harvesting antennae based on the irradiance level received by the cells is in good agreement with a previous study carried out with *A. carterae* (Ruivo et al., 2011). The exceptions to this pattern were the minority photoprotective pigments pyrrhoxanthin and diatoxanthin, neither of which showed any clear trend (see Fig. 4). Photoprotective pigments allow excess energy to be regulated as a result of heat dissipation. Since the Y_o levels assayed were not photoinhibitory for *A. carterae*, as reported previously (Molina-Miras et al., 2018), the cells did not compel their photoprotective machinery.

Nutrient availability also influenced pigment synthesis. Thus, the increased nutrient concentrations in the culture medium from $f/2 \times 1$ in set 4 to $f/2 \times 3$ in set 6 resulted in greater cellular pigment contents, except for the minor pigment pyrrhoxanthin, the effect on which was not significant. These results are in line with others published previously for the dinoflagellate *Heterocapsa* sp. (Latasa and Berdalet, 1994). The intracellular concentration of the pigments chl-a, chl-c, peridinin, diadinoxanthin, diatoxanthin and β -carotene in *Heterocapsa* sp. declined when cultured in batch mode under deficiency of nitrogen and phosphorus (Latasa and Berdalet, 1994).

In spite of the great diversity of microalgal carotenoid pigments reported, only a few, including β -carotene, astaxanthin, lutein, canthaxanthin and fucoxanthin, are currently of commercial interest (Gong and Bassi, 2016). However, the majority of industrially produced carotenoids are synthesized chemically, and of the small portion marketed from natural sources, microalgae are still at a disadvantage with respect to plants in cases such as lutein. The advantages, disadvantages and future of non-dinoflagellate microalgae as a carotenoid source have been comprehensively discussed in recent reviews (Gong and Bassi, 2016). Dinoflagellates only produce two of the above-mentioned five carotenoids, namely β -carotene and fucoxanthin. With the titers achieved herein for these two pigments, it is improbable that marine dinoflagellates could compete with non-dinoflagellate microalgae, at least in the short term. Notwithstanding this, enhanced biomass yields in the mass culture of a few dinoflagellate species in photobioreactors have recently allowed a scale-up to a pilot-scale level to produce high-value bioactive substances (Jaufrays et al., 2012; López-Rosales et al., 2017; Molina-Miras et al., 2018). In this scenario, pigments are generated as co-products and should, in general, be extracted to improve the economics and sustainability of these bioprocesses, as occurs in the case of microalgae-based biorefineries (Chew et al., 2017). The

carotenoids from *A. carterae* only present in dinophytes (i.e. peridinin, pyrrhoxanthin and peridininol, as far as we know) deserve special attention due to the absence of alternative non-microbial natural sources. The most representative of these is peridinin. *A. carterae* is also an important source of peridinin-chlorophyll-a-protein, PCPs (Carbonera et al., 2014). The peridinin content achieved herein ranged from 0.2% to 0.9% of biomass dry weight, which falls within the ranges reported for other dinoflagellates (Johansen et al., 1974; Benstein et al., 2014). The maximum peridinin titer ($4.44 \pm 0.31 \text{ mgL}^{-1}$) was obtained in Set 6, with an average production rate of $19.4 \pm 1.35 \text{ mg m}^{-2} \text{ L}^{-1}$. This peridinin productivity is similar to the maximum value reported for the dinoflagellate *Symbiodinium voratum* when grown immobilized in a bench-scale twin-layer PBR (Benstein et al., 2014). The maximum productivities for the other minor carotenoids were well below that for peridinin. However, it should be taken into account that the optimal abiotic stresses maximizing the cell synthesis of metabolites may differ depending on the metabolite in question (Paliwal et al., 2017). Indeed, this is the case for *A. carterae* in this study, where the predicted optimal operating conditions for bioactive macrolides and carotenoids were not entirely coincident. If they were, cell carotenoids could markedly increase as well. For example, elevated shear regimens enhanced the cell-specific production of the yessotoxins, peridinin and dinoxanthin in the marine dinoflagellate *Protoceratium reticulatum* as long as the intensity of the shear stress was insufficient to kill the cells outright (Rodríguez et al., 2009)

3.4. Fatty acids

Fig. 5 shows radar plots profiling mean levels of the saponifiable fatty acids (FAs) determined in the biomass of *A. carterae* cultured in semicontinuous mode (Sets 3–7). The FAs quantified comprised tetradecanoic acid (14:0), hexadecanoic acid (16:0), octadecanoic acid (C18:0), oleic acid (18:1n9), 9-eicosenoic acid (20:1n9), stearidonic acid (SDA; 18:4n3), EPA (20:5n3) and DHA (22:6n3). The total FA content (FA_T) was not significantly affected by the environmental conditions tested in the semicontinuous cultures (Set 3–7), with an average FA_T value of $13.0 \pm 0.9\%$ d.w. for all sets. FAs were grouped

into three classes, namely saturated (SFAs), monounsaturated (MUFAs) and polyunsaturated (PUFAs) fatty acids (Fig. 5A). Irrespective of the set considered, the majority of SFA was 16:0 (Fig. 5B); the dominant MUFA was 18:1n9, whereas proportions of 20:1n9 were always low (Fig. 5C). *A. carterae* was always rich in SDA, EPA and DHA (Fig. 5D). The PUFA fraction was always higher than 56% of the FA_T , except in Set 4. This profile exhibited by *A. carterae* is in line with others reported previously for the same species grown photoautotrophically (Bigogno et al., 2002; Mansour et al., 2005).

The variations in the *A. carterae* fatty acid profile (relative to both biomass dry weight and total saponifiable fatty acids), together with the availability of nutrients in the culture medium and irradiance, followed a general pattern that is well-established in the literature (Reitan et al., 1994; Khoeyi et al., 2012). Thus, in the transition from Set 4–6 (nutrients in the culture medium increased from $f/2 \times 1$ to $\times 3$ (see Table 1)), relative levels of SFAs and MUFAs (mainly 18:1n9) declined as nutrient concentration increased, whereas the relative amounts of PUFAs increased (see Fig. 5), as observed previously for other species (Reitan et al., 1994). In contrast, in the transitions from Set 3–4 and from Set 6–7, which are characterized by an increase in the daily irradiance (Y_o in Table 1), the relative amounts of PUFAs and SFAs decreased and increased respectively (more strongly from Set 3–4) (see Fig. 4). An exception was found for the DHA content, which increased slightly with Y_o , as also observed for several dinoflagellate microalgae (Zhukova and Titlyanov, 2006). The maximum PUFA productivity of biomass was found in Set 7, with an average value of $2.19 \pm 0.55 \text{ mgL}^{-1} \text{ day}^{-1}$ and mean EPA and DHA contents with respect to biomass dry weight of $1.69 \pm 0.31\%$ d.w. and $3.47 \pm 0.24\%$ d.w.

3.5. Future prospects

In essence, the culture system developed in this study can be extended to production of bioactives and metabolites obtained from microalgal dinoflagellate-based bioprocesses. A paddlewheel-driven raceway PBR may be effectively used up to a working volume from several hundred to thousand liters to grow photoautotrophically a

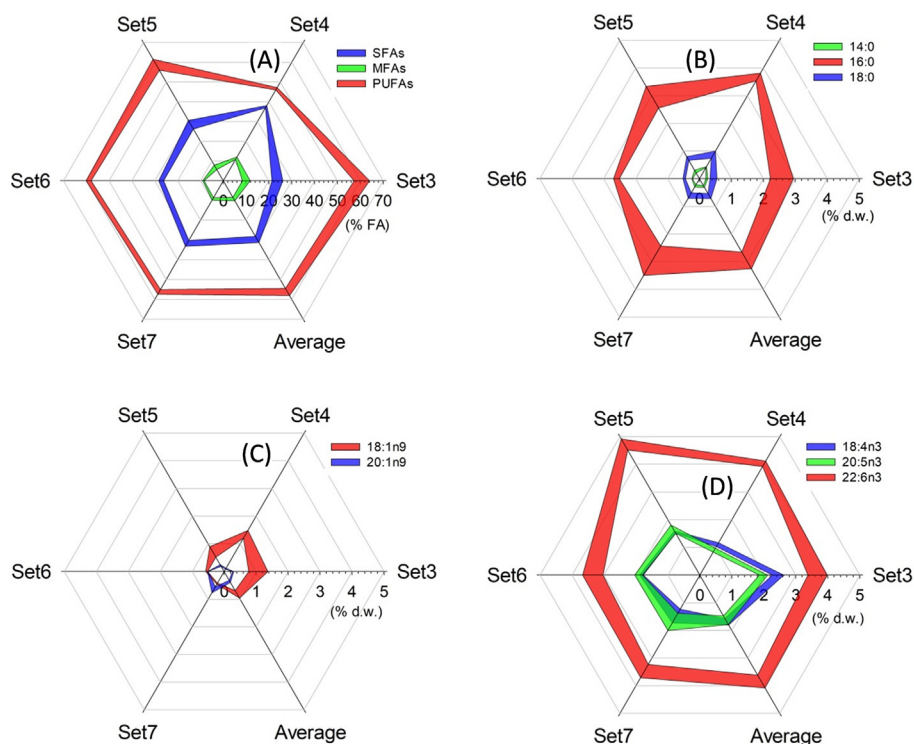


Fig. 5. Radar plots depicting profile and distribution of the saponifiable fatty acids from *A. carterae* in the experimental sets corresponding to semicontinuous cultures (sets 3–7). (A) Percentages of saturated (SFAs), monounsaturated (MUFAs) and polyunsaturated (PUFAs) fatty acids with respect to the total saponifiable fatty acid content in the biomass (FA). Percentage of individual fatty acids with respect to biomass dry weight: (B) SFAs; (C) MUFAs; (D) PUFAs.

shear-sensitive dinoflagellate such as *Amphidinium carterae*. Although the cultivation of dinoflagellates for potentially commercial applications is becoming increasingly popular, algal biomass thereof is mainly processed to the currently known metabolites. By contrast, supernatants are virtually unexploited, despite it is well-known that dinoflagellates release dissolved organic matter (DOM) during their growth. DOM from dinoflagellates cultures may be a source of attractive bioactive substances and/or also provide nutrients or growth promoters for the cells themselves. Therefore, future research should be aimed at the application of spent media recycle strategies for identifying high value products from chemical characterization of DOM and for later recovery. The supernatant recycle would also have significant economic and environmental benefits. Since the uptake of DOM by dinoflagellates via osmotrophy, mixotrophy or heterotrophy is another issue that deserves to be explored, the application of synergistic systems of dark fermentation and algal culture, as recently proposed for non-dinoflagellate microalgae (Ren et al., 2018), may result particularly interesting.

4. Conclusions

The long-term culture of a dinoflagellate in a raceway PBR has been demonstrated for the first time. Semicontinuous mode was a better and robust operational mode for using with *Amphidinium carterae*. A culture medium with the composition $f/2 \times 3$ (N:P = 5), combined with a sinusoidal irradiance pattern (L/D cycle of 24:0) and an I_{max} of $900 \mu E m^{-2} s^{-1}$, provided the best results. Carotenoids and polyunsaturated fatty acids were produced in sufficient amounts to be considered as valuable subproducts. The culture methodology described is an attractive approach for the continuous, reliable and sustainable supply of dinoflagellate biomass in uniform quality and yield.

Acknowledgments

This research was funded by the Spanish Ministry of Economy and Competitiveness (CTQ2014-55888-C3-02) and the European Regional Development Fund Program.

Appendix A. Supplementary data

Supplementary data associated with this article can be found, in the online version, at <https://doi.org/10.1016/j.biortech.2018.05.104>.

References

- Adarme-Vega, T.C., Thomas-Hall, S.R., Schenk, P.M., 2014. Towards sustainable sources for omega-3 fatty acids production. *Curr. Opin. Biotechnol.* 26, 14–18.
- Assunção, J., Guedes, A., Malcata, F.X., 2017. Biotechnological and pharmacological applications of biotoxins and other bioactive molecules from dinoflagellates. *Mar. Drugs* 15 (12), 393.
- Benstein, R.M., Çebi, Z., Podola, B., Melkonian, M., 2014. Immobilized growth of the peridinin-producing marine dinoflagellate *Symbiodinium* in a simple biofilm photobioreactor. *Mar. Biotechnol.* 16 (6), 621–628.
- Bigogno, C., Khozin-Goldberg, I., Boussiba, S., Vonshak, A., Cohen, Z., 2002. Lipid and fatty acid composition of the green oleaginous alga *Parietochloris incisa*, the richest plant source of arachidonic acid. *Phytochemistry* 60 (5), 497–503.
- Burkhardt, S., Zondervan, I., Riebesell, U., 1999. Effect of CO₂ concentration on C:N:P ratio in marine phytoplankton: a species comparison. *Limnol. Oceanogr.* 44 (3), 683–690.
- Camacho, F.G., Rodríguez, J.G., Mirón, A.S., García, M.C.C., Belarbi, E.H., Chisti, Y., Grima, E.M., 2007. Biotechnological significance of toxic marine dinoflagellates. *Biotechnol. Adv.* 25 (2), 176–194.
- Carbonera, D., Di Valentin, M., Spezia, R., Mezzetti, A., 2014. The unique photophysical properties of the Peridinin-Chlorophyll-a-Protein. *Curr. Protein Pept. Sci.* 15 (4), 332–350.
- Chew, K.W., Yap, J.Y., Show, P.L., Suan, N.H., Juan, J.C., Ling, T.C., Lee, D.-J., Chang, J.-S., 2017. Microalgae biorefinery: high value products perspectives. *Bioresour. Technol.* 229, 53–62.
- Finkel, Z., Quigg, A., Raven, J., Reinfelder, J., Schofield, O., Falkowski, P., 2006. Irradiance and the elemental stoichiometry of marine phytoplankton. *Limnol. Oceanogr.* 51 (6), 2690–2701.
- Fuentes-Grunewald, C., Bayliss, C., Fonluf, F., Chapuli, E., 2016. Long-term dinoflagellate culture performance in a commercial photobioreactor: *Amphidinium carterae* case. *Bioresour. Technol.* 218, 533–540.
- Gallardo-Rodríguez, J., Sánchez-Mirón, A., García-Camacho, F., López-Rosales, L., Chisti, Y., Molina-Grima, E., 2012. Bioactives from microalgal dinoflagellates. *Biotechnol. Adv.* 30 (6), 1673–1684.
- García-Camacho, F., Sánchez-Mirón, A., Gallardo-Rodríguez, J., López-Rosales, L., Chisti, Y., Molina-Grima, E., 2014. Culture of microalgal dinoflagellates. In: Botana, L.M. (Ed.), *Seafood and Freshwater Toxins: Pharmacology, Physiology, and Detection*, third ed. CRC Press, Boca Raton, pp. 551–566.
- Gong, M., Bassi, A., 2016. Carotenoids from microalgae: a review of recent developments. *Biotechnol. Adv.* 34 (8), 1396–1412.
- Henriksen, P., Riemann, B., Kaas, H., Sørensen, H.M., Sørensen, H.L., 2002. Effects of nutrient-limitation and irradiance on marine phytoplankton pigments. *J. Plankton Res.* 24 (9), 835–858.
- Huesemann, M., Dale, T., Chavis, A., Crowe, B., Twary, S., Barry, A., Valentine, D., Yoshida, R., Wigmosta, M., Cullinan, V., 2017. Simulation of outdoor pond cultures using indoor LED-lighted and temperature-controlled raceway ponds and Phenometrics photobioreactors. *Algal Res.* 21, 178–190.
- Ishikawa, C., Jomori, T., Tanaka, J., Senba, M., Mori, N., 2016. Peridinin, a carotenoid, inhibits proliferation and survival of HTLV-1-infected T-cell lines. *Int. J. Oncol.* 49 (4), 1713–1721.
- Jauffrais, T., Kilcoyne, J., Séchet, V., Herrenknecht, C., Truquet, P., Hervé, F., Bérard, J.B., Nulty, C., Taylor, S., Tillmann, U., 2012. Production and isolation of azaspiracid-1 and-2 from *Azadinium spinosum* culture in pilot scale photobioreactors. *Mar. Drugs* 10 (6), 1360–1382.
- Jeffrey, S., 1997. Chlorophyll and carotenoid extinction coefficients. *Phytoplankton pigments in oceanography: guidelines to modern methods*. UNESCO, Paris 595–596.
- Jeffrey, S., Wright, S., 2006. Photosynthetic pigments in marine microalgae: insights from cultures and the sea. *Algal cultures, Analogues of blooms and applications 1*, 33–90.
- Johansen, J., Svech, W., Liaaen-Jensen, S., Haxo, F., 1974. Carotenoids of the dinophyceae. *Phytochemistry* 13 (10), 2261–2271.
- Khoeyi, Z.A., Seyfabad, J., Ramezanzpour, Z., 2012. Effect of light intensity and photo-period on biomass and fatty acid composition of the microalgae, *Chlorella vulgaris*. *Aquacult. Int.* 20 (1), 41–49.
- Latasa, M., Berdalet, E., 1994. Effect of nitrogen or phosphorus starvation on pigment composition of cultured *Heterocapsa* sp. *J. Plankton Res.* 16 (1), 83–94.
- Leonardos, N., Geider, R.J., 2004. Effects of nitrate: phosphate supply ratio and irradiance on the C:N:P stoichiometry of *Chaetoceros muelleri*. *Eur. J. Phycol.* 39 (2), 173–180.
- López-Rosales, L., García-Camacho, F., Sánchez-Mirón, A., Beato, E.M., Chisti, Y., Grima, E.M., 2016. Pilot-scale bubble column photobioreactor culture of a marine dinoflagellate microalga illuminated with light emission diodes. *Bioresour. Technol.* 216, 845–855.
- López-Rosales, L., García-Camacho, F., Sánchez-Mirón, A., Contreras-Gómez, A., Molina-Grima, E., 2015. An optimisation approach for culturing shear-sensitive dinoflagellate microalgae in bench-scale bubble column photobioreactors. *Bioresour. Technol.* 197, 375–382.
- López-Rosales, L., Sánchez-Mirón, A., García-Camacho, F., Place, A., Chisti, Y., Molina-Grima, E., 2017. Pilot-scale outdoor photobioreactor culture of the marine dinoflagellate *Karlodinium veneticum*: Production of a karlotoxins-rich extract. *Bioresour. Technol.*
- Mansour, M.P., Frampton, D.M., Nichols, P.D., Volkman, J.K., Blackburn, S.I., 2005. Lipid and fatty acid yield of nine stationary-phase microalgae: applications and unusual C24–C28 polyunsaturated fatty acids. *J. Appl. Phycol.* 17 (4), 287–300.
- Molina-Miras, A., Morales-Amador, A., de Vera, C., López-Rosales, L., Sánchez-Mirón, A., Souto, M., Fernández, J., Norte, M., García-Camacho, F., Molina-Grima, E., 2018. A pilot-scale bioprocess to produce amphidinols from the marine microalga *Amphidinium carterae*: isolation of a novel analogue. *Algal Res.* 31, 87–98.
- Ondera, K.-I., Konishi, Y., Taguchi, T., Kiyoto, S., Tominaga, A., 2014. Peridinin from the marine symbiotic dinoflagellate, *Symbiodinium* sp., regulates eosinophilia in mice. *Mar. Drugs* 12 (4), 1773–1787.
- Paliwal, C., Mitra, M., Bhayani, K., Bharadwaj, S.V., Ghosh, T., Dubey, S., Mishra, S., 2017. Abiotic stresses as tools for metabolites in microalgae. *Bioresour. Technol.*
- Parsons, T., Stephens, K., Strickland, J., 1961. On the chemical composition of eleven species of marine phytoplankters. *J. Fish. Board Can.* 18 (6), 1001–1016.
- Reitan, K.I., Rainuzzo, J.R., Olsen, Y., 1994. Effect of nutrient limitation on fatty acid and lipid content of marine microalgae. *J. Phycol.* 30 (6), 972–979.
- Ren, H.Y., Kong, F., Ma, J., Zhao, L., Xie, G.J., Xing, D., Guo, W.Q., Liu, B.F., Ren, N.Q., 2018. Continuous energy recovery and nutrients removal from molasses wastewater by synergistic system of dark fermentation and algal culture under various fermentation types. *Bioresour. Technol.* 252, 110–117.
- Reynolds, R.A., Stramski, D., Kiefer, D.A., 1997. The effect of nitrogen limitation on the absorption and scattering properties of the marine diatom *Thalassiosira pseudonana*. *Limnol. Oceanogr.* 42 (5), 881–892.
- Rodríguez-Ruiz, J., Belarbi, E.-H., Sánchez, J.L.G., Alonso, D.L., 1998. Rapid simultaneous lipid extraction and transesterification for fatty acid analyses. *Biotechnol. Tech.* 12 (9), 689–691.
- Rodríguez, J., Mirón, A.S., Camacho, F.G., García, M., Belarbi, E., Chisti, Y., Grima, E.M., 2009. Causes of shear sensitivity of the toxic dinoflagellate *Protoceratium reticulatum*. *Biotechnol. Prog.* 25 (3), 792–800.
- Ruivo, M., Amorim, A., Cartaxana, P., 2011. Effects of growth phase and irradiance on phytoplankton pigment ratios: implications for chemotaxonomy in coastal waters. *J. Plankton Res.* 33 (7), 1012–1022.
- Sakshaug, E., Andresen, K., Mykkestad, S., Olsen, Y., 1983. Nutrient status of phytoplankton communities in Norwegian waters (marine, brackish, and fresh) as revealed by their chemical composition. *J. Plankton Res.* 5 (2), 175–196.
- Sakshaug, E., Granéli, E., Elbrächter, M., Kayser, H., 1984. Chemical composition and alkaline phosphatase activity of nutrient-saturated and P-deficient cells of four

- marine dinoflagellates. *J. Exp. Mar. Biol. Ecol.* 77 (3), 241–254.
- Sánchez Mirón, A., Garcia Camacho, F., Contreras Gomez, A., Grima, E.M., Chisti, Y., 2000. Bubble column and airlift photobioreactors for algal culture. *AIChE J.* 46 (9), 1872–1887.
- Seoane, S., Zapata, M., Orive, E., 2009. Growth rates and pigment patterns of haptophytes isolated from estuarine waters. *J. Sea Res.* 62 (4), 286–294.
- Van de Waal, D.B., Smith, V.H., Declerck, S.A., Stam, E., Elser, J.J., 2014. Stoichiometric regulation of phytoplankton toxins. *Ecol. Lett.* 17 (6), 736–742.
- Wang, S., Chen, J., Li, Z., Wang, Y., Fu, B., Han, X., Zheng, L., 2015. Cultivation of the benthic microalga *Prorocentrum lima* for the production of diarrhetic shellfish poisoning toxins in a vertical flat photobioreactor. *Bioresour. Technol.* 179, 243–248.
- Zapata, M., Rodríguez, F., Garrido, J.L., 2000. Separation of chlorophylls and carotenoids from marine phytoplankton: a new HPLC method using a reversed phase C8 column and pyridine-containing mobile phases. *Mar. Ecol. Prog. Ser.* 29–45.
- Zhukova, N.V., Titlyanov, E.A., 2006. Effect of light intensity on the fatty acid composition of dinoflagellates symbiotic with hermatypic corals. *Bot. Mar.* 49 (4), 339–346.